8 Appendix

This is a selected list of appendices; these are the most informative or have been evaluated as critical to the text. A number of other supporting information is attached on the accompanying CD.

8.1 List of printed appendices

Appendix 1. Information on the Bch-1 core

Appendix 2. Geochemistry calibrations

Appendix 3. Magnetic Susceptibility calibration

Appendix 4. Sedimentation rate model

8.2 List of CD content

Appendix 1. Information on the Bch-1 core

Appendix 2. Geochemistry calibrations

Appendix 3. Magnetic Susceptibility calibration

Appendix 4. Sedimentation rate model

Appendix 5. EHA of the MS and grayscale

Appendix 7. Sample positions

Appendix 8. Frequency dependent MS

Appendix 1. Information on the Bch-1 core

This project was funded by grant GACR grant number P210/10/1991 Principal Investigator RNDr D. Uličný CSc.

The Bch-1 drill site is positioned at 50°18´54.2´´N and 15°17´42.03´´E, the core reached 405 m. The lithology was originally described by Mgr. S. Čech and RNDr. D. Uličný, CSc. The core was drilled by the wireline technique and is six centimetres in diameter, with a recovery rate exceeding 90 %.

Fig Ap.1
The washed core as photographed for the purposes of grayscale extraction. One of the light coloured Lithotype III beds displayed as well as a bioclastic fragment above. Note the almost imperceptible hairline crack between the two separate peaces; this was the case for most of the core allowing for an acquisition of unbroken grayscale record.

Appendix 2. Geochemistry Calibrations

Calibration equations of XRF geochemistry datasets, are courtesy of Mgr. Jiří Laurin, Ph.D.

Dataset 1:

XRF analysis performed at the Institute of Inorganic Chemistry, AS CR; calibration equations supplied by the Institute of Inorganic Chemistry, AS CR

Al_{CAL} (wt.%) = -0.0000789*(Al_{XRF} ^2) + 0.044* Al_{XRF} - 0.244

Si_{CAL} (wt.%) = 0.0261* Si_{XRF} - 0.5447

Ca_{CAL} (wt.%) = -0.00000001*(Ca_{XRF} ^2) + 0.0018* Ca_{XRF} + 1.3985

Ti_{CAL} (wt.%) = -0.0000039*(Ti_{XRF} ^2) + 0.0021* Ti_{XRF}

Zr_{CAL} (wt.%) = -0.000000155*(Zr_{XRF} ^2) + 0.000201* Zr_{XRF}

Dataset 2:

XRF analysis performed at the Institute of Geophysics, AS CR, using a handheld XRF analyzer. Zr, Ti and Al calibrations based on ICP MS analysis (SGS, Toronto), Ca and Si calibrated with the classical silicate-rock analysis (Geological Survey, Prague).

Zr_{CAL} (wt.%) = 0.0009*(Zr_{XRF} ^2) + 0.4593* Zr_{XRF}

Al_{CAL}(wt.%)=0.0418*(Al_{XRF}^2)+0.8454*Al_{XRF}

Ti_{CAL} (wt.%) = -1.242*(Ti_{XRF} ^2) + 1.238* Ti_{XRF}

Ca_{CAL} (wt.%) = -0.0058*(Ca_{XRF} ^2) + 0.8607* Ca_{XRF} + 6.5568

Si_{CAL} (wt.%) = 0.0091*(Si_{XRF} ^2) + 0.2523* Si_{XRF} + 5.4067

Appendix 3. Kappameter calibration

The Kappameter dataset has proven different in value to Kappabridge measurements; this is to some degree unresolved as both devices should give the same value. The difference probably lies in the automatic core correction or a wrong entry of the diameter value. The Kappabridge dataset appears to be more precise and they were taken as a standard; fortunately the relationship between both methods are strictly linear, see ***fig Ap.4*** , therefore a simple re-calculation was adopted.

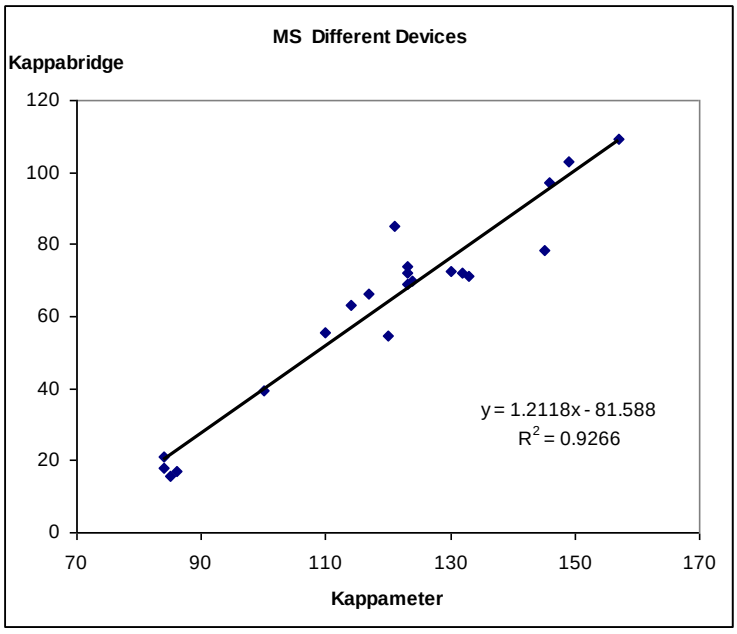

Fig Ap.4
Showing correlation between the 21 correction samples and their counterparts in the Kappameter series showing a good correlation, however the data do display different MS as can be seen from the x and y axis values, The ensuing procedure therefore was to reduce the value of original log based on the equation of linear regression.

Equation:

The value of coefficient of determination for linear least square regression is 0.93 which is considered a very good fit (*e.g. Mayer & Appel, 1999*). The mismatch in total MS value was probably caused by discrepancies connected to the core size correction.

Appendix 4. Sedimentation rate model

Sedimentation rate estimates were calculated using the biostratigraphic and carbon-isotope markers, see **Tab Ap.5**. Some of them have been pinpointed on the core, others have been correlated from the surrounding cores (marked in red colour). The floating time scale has been incorporated from Laurin et al. (*in prep.*)

Tab Ap.5

Marker	Floating time scale [kyr]
FO C. crassus	-241
Navigation Event	0
Did I	130
FO P. germari	340
FO M. scupini	705
Bridgewick Event	1255
FO I.perplexus	1459
Pewsey Event	1500
Glynde Event	1788

The resultant sedimentation rate model is shown on the **fig A.5,** which shows the intervals between two consecutive markers and the calculated sedimentation rate (dark blue lines) plus a model situation where continuous sedimentation without major jumps in sedimentation Rate is expected (aqua colour trend).

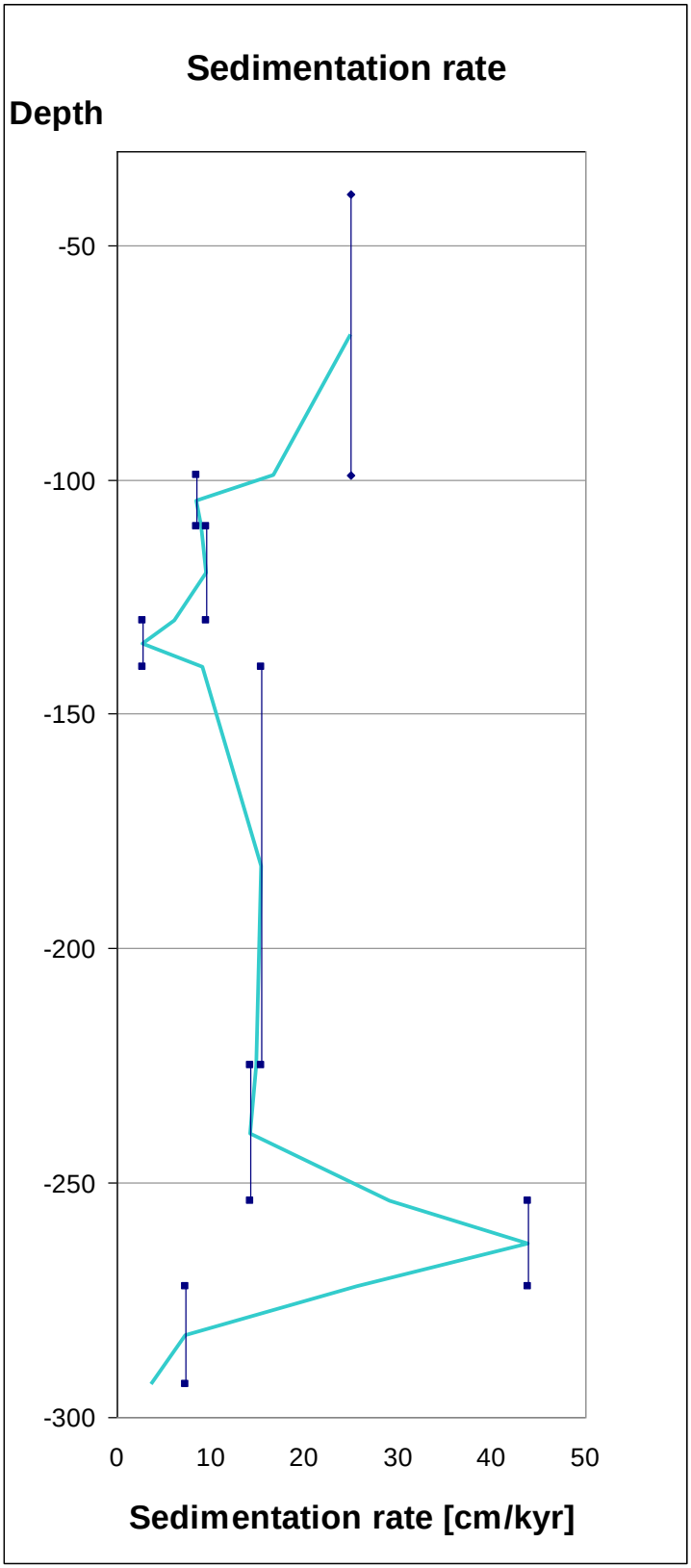

Appendix 5.

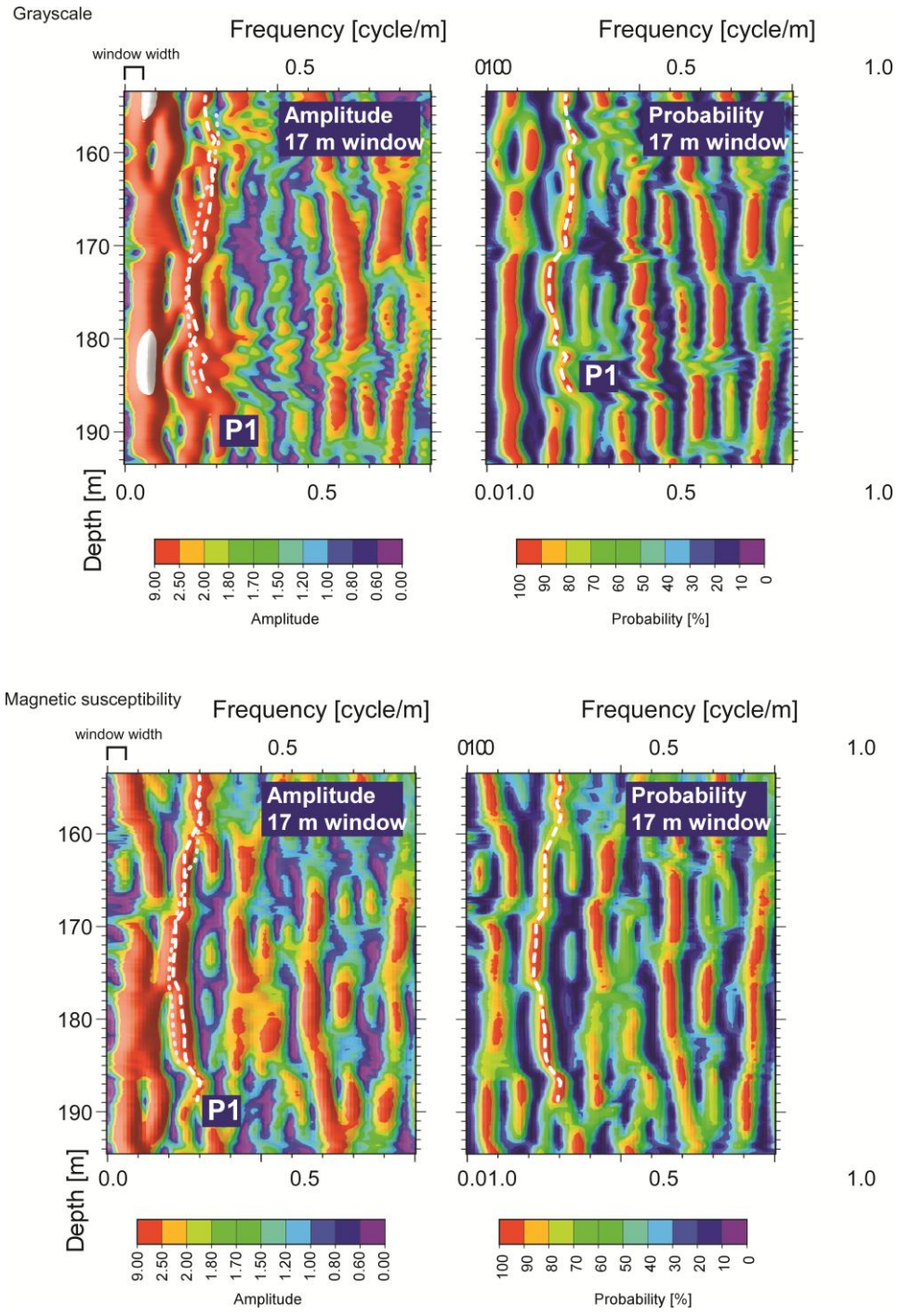

The EHA results for tuned Magnetic susceptibility and grayscale with marked position of the precession signal.

Appendix 6. Sample positions

Microscopy

The inspected 24 thin sections were partly adopted from the original Bch-1 investigation (6 samples) and an additional 18 samples were carefully selected mainly to reflect variations in Litholoty II and III.

Lithology 0 : 205.02 m, 214.52 m

Lithology I : 185.41 m, 185.52 m, 188.66 m, 189.57 m, 199.04 m

Lithology II : 146.08 m, 146.55 m, 155.31 m, 163.12 m, 163.32 m, 167.02 m, 171.85 m, 172.94 m, 177.29 m, 177.72 m, 179.53 m, 181.35 m,

Lithology III : 158.5 m, 163.18 m, 172.05 m, 177.53 m, 182.57 m

Niton geochemistry

The samples were designed to track the difference between Lithotype II and III and what appeared to be its counterpart in Lithotype I.

Lithotype 0 : 202 m, 209 m, 220.5 m

Lithotype I : 186.3 m, 186,7 m 187 m

Lithotype II : 147.8 m, 158.75 m, 171.85 m, 172.94 m

Lithotype III : 148 m, 158.5 m, 172 m

Magnetic susceptibility

The collected 21 control samples were picked to reflect the extreme Kappameter value positions as well as the respective Lithotypes. The 18 microscope samples plus three additional were used.

Lithology 0 : 200.75 m, 202 m

Lithology I : 185.41 m, 185.52 m, 188.66 m, 189.57 m

Lithology II : 146.08 m, 146.55 m, 155.31 m, 163.12 m, 163.32 m, 171.85 m, 172.94 m, 177.29 m, 177.72 m, 181.35 m, 182.57 m

Lithology III : 163.18 m, 172.05 m, 177.53 m, 182.57 m

Palynomorph data

Six samples were collected in order to ascertain T:M ratio changes between the Lithotype II and III.

Lithotype II : 172.94 m, 163.12 m

Lithotype III : 163.18 m , 172.05 m, 181.35 m, 182.57 m

Appendix 7. Frequency dependent MS

A frequency-dependent MS was acquired for the 21 leading samples.

A frequency-dependent MS can be ascertained on MFK-1; this is traditionally interpreted as resulting from interplay between superparamagnetic (e.g. diagenetic magnetite) and stable single domain (e.g. magnetofossil magnetite) or even multidomain magnetic particles (e.g. detrital magnetite). This approach was pioneered by Dearing et al. in (1996) (*for a review see Pokorný et al., 2011*), who introduced the following commonly accepted parameter.

$$\chi_{FD} = \frac{\chi_{LF} - \chi_{HF}}{\chi_{LF}} \cdot 100\%$$

Where χ_{LF} and χ_{HF} are susceptibilities measured at the lower and higher frequencies respectively.

Fig Ap.8
Shows the variation of the frequency dependent susceptibility with the depth of the borehole. This means there must be some minor admixture of ultrafine magnetite.

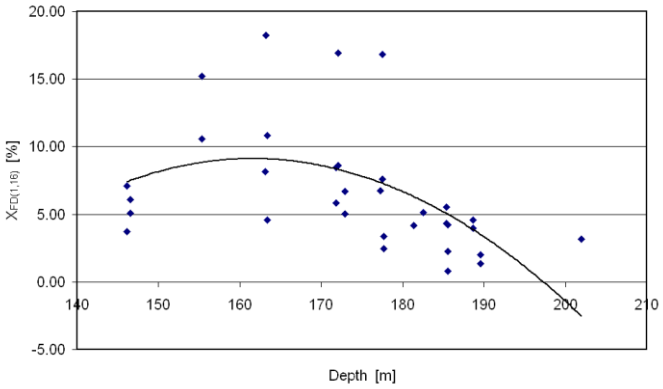

From frequency dependence of MS, see ***fig s***; it is obvious that the X_{FD} parameter is relatively low at the depth below 150 m. In the depth interval between 150 m and 180 m it is varied, showing the values between 5% and 20% and below 180 m it is again low falling even under 5%.

This behaviour can be interpreted in two ways. First, the amount of ultrafine SP particles initially increased and then became variable before finally decreasing due to sedimentological processes. Second, the SP particles are diagenetic in origin and their amount is governed by post-sedimentary environmental conditions.

It is an unequivocal proof that some ferromagnetic constituents are present, however, as it has been proven that majority of the MS signal was carried by paramagnetic minerals, it just remains another piece of the puzzle to be addressed. As the origin of the ultrafine magnetite remains obscure the results were not interpreted for the purpose of the thesis.